

# Enabling Mobile Base Stations in 5G via Wireless Access Backhaul (WAB): A Multi-Band Experimental Study

Chiara Rubaltelli, Marcello Morini, Eugenio Moro, Ilario Filippini

Dipartimento di Elettronica, Informazione e Bioingegneria, Politecnico di Milano, Milan, Italy

$\langle name \rangle.\langle surname \rangle@polimi.it$

**Abstract**—Highly dynamic and mobile applications, such as vehicular networks, require stable connectivity, which is often challenging to achieve. Network densification is a key approach to address this issue and can be achieved cost-effectively through mobile base stations and wireless relaying. However, existing solutions rely on rigid and complex architectures that hinder deployment in dynamic scenarios. The recently standardized Wireless Access Backhaul (WAB) architecture represents a key evolution, enabling flexible and modular wireless relay networks with native support for mobility and multi-technology wireless backhaul. This paper presents the first experimental realization of a multi-band WAB testbed, combining an FR2 backhaul and an FR1 access link using open-source software and commercial off-the-shelf components. The proposed framework validates end-to-end WAB operation under mobility and demonstrates the extension of FR2 coverage while maintaining compatibility with legacy FR1 user equipment. Experimental campaigns in vehicular and outdoor-to-indoor scenarios confirm that WAB effectively mitigates FR2 limitations, particularly in uplink and Non-Line-of-Sight conditions. These results highlight WAB as a practical and scalable approach for vehicular and next-generation wireless networks.

**Index Terms**—Wireless Access and Backhaul (WAB), moving networks, mobile cells, FR1/FR2 system, 3GPP RAN architectures, SDR testbed.

## I. INTRODUCTION

The growing demand for bandwidth and spectral efficiency in wireless networks has intensified research into new frequency bands and novel Radio Access Network (RAN) architectures for 5G. Network *densification* is a key enabler to sustain this continuous growth in radio access capacity demand, particularly in urban vehicular environments. Such environments are characterized by high user mobility, rapidly varying traffic conditions, and bandwidth-intensive applications such as autonomous driving, which require high-data-rate video streams. Densification also facilitates the adoption of higher frequency bands for radio access, such as Frequency Range 2 (FR2, 24.25–71 GHz), which offers wide bandwidths and supports multi-Gbps data rates, but suffers from severe path loss, high penetration losses, and strong susceptibility to environmental dynamics. These effects are particularly pronounced in vehicular scenarios [1].

To mitigate the deployment costs associated with dense infrastructure in vehicular networks, *wireless relaying* provides a cost-effective means to increase the number of Base Stations (BSs). Furthermore, Mobile Base Stations (MBSs) represent a

promising solution to address the strong temporal and spatial variability of traffic demand in vehicular environments and to explore further cost–capacity trade-offs. Indeed, as shown in [2], substantial cost savings can be achieved by deploying MBSs in place of static ones. Consequently, a mobility-capable radio access infrastructure based on wireless relaying becomes particularly attractive for vehicular and dynamic urban scenarios, where rapid reconfiguration and service continuity under mobility are essential.

To enable effective wireless relaying, 3rd Generation Partnership Project (3GPP) took an initial step in 2019 by introducing Integrated Access and Backhaul (IAB) in Release 15, based on the wireless backhaul paradigm. Several enhancements have been proposed in subsequent releases to improve the technology; however, IAB has not achieved widespread adoption yet. The intrinsic complexity of the IAB architecture, together with its limited flexibility, makes it poorly suited to highly dynamic scenarios, such as vehicular networks and mobile base station deployments, which demand frequent backhaul reconfiguration and seamless backhaul handovers under mobility.

For these reasons, the Mobile Base Station Relay (MBSR) topic has quickly gained momentum within IAB studies, resulting in the introduction and standardization of Wireless Access Backhaul (WAB) in Release 19 [3]. WAB leverages the benefits of wireless backhaul while relying on standard 5G components and procedures, thereby enabling a rapid and cost-efficient deployment. Each WAB node integrates a Mobile Termination (MT) with a complete Next Generation NodeB (gNB), enabling direct access to User Equipments (UEs) and seamless backhaul handovers.

Furthermore, the modular design of WAB supports multiple backhaul technologies, including Non-Terrestrial Networks (NTNs), and introduces full independence between the access and backhaul segments. This feature enables WAB deployments in highly dynamic environments, such as trains, ships, and airplanes, where terrestrial backhaul availability is limited or discontinuous.

In this context, WAB represents a promising evolution in the field of MBSs. However, to date, no physical implementation has been publicly documented. This paper addresses this gap by presenting a multi-band WAB testbed that integrates a commercial backhaul with an access segment using open-source

software, Software-defined Radios (SDRs), and commercial components. Leveraging the multi-technology capabilities of WAB, the proposed solution combines the high throughput offered by FR2 communications in the backhaul with the wider device compatibility and superior penetration of Frequency Range 1 (FR1, 410–7125 MHz) in the access segment. The proposed testbed, assembled from Commercial Off-the-Shelf (COTS) components, demonstrates that the implementation of a WAB architecture can be achieved rapidly and cost-effectively using existing technological expertise. These results suggest that the widespread adoption of WAB may be closer to realization than previously anticipated.

Using this testbed, we conducted an experimental campaign to validate the proposed system in urban vehicular and Outdoor to Indoor (O2I) scenarios, confirming its potential to extend the benefits of FR2 communications by mitigating typical FR2 propagation impairments. This initial campaign highlights the main advantages of wireless backhaul. In particular, the results demonstrate that WAB nodes can maintain robust connectivity under mobility. Moreover, the WAB architecture effectively overcomes uplink transmission limitations, providing enhanced performance even in challenging Non-Line of Sight (NLoS) indoor environments.

The main contributions of this work can be summarized as follows:

- We provide an overview and discussion of the WAB architecture as a key enabler for mobility-aware and vehicular mobile base station deployments.
- We present, to the best of our knowledge, the first physical implementation of the WAB architecture, realizing a complete multi-band testbed that combines a commercial FR2 wireless backhaul with an FR1 access segment based on open-source software.
- We experimentally validate the proposed system in realistic urban vehicular and O2I scenarios, demonstrating robust connectivity under mobility and improved performance in challenging propagation conditions.

The remainder of this paper is organized as follows. Section II reviews the related work. Section III outlines the WAB architecture and its fundamental operations. Section IV details the proposed multi-band testbed and its main components. Section V presents the experimental campaign and discusses the obtained results. Finally, Section VI concludes the paper and highlights future research directions.

## II. BACKGROUND ON WIRELESS BACKHAUL

Prior to WAB, 3GPP standardized several wireless relay architectures. Introduced in Release 15 [4], IAB enables wireless backhaul and supports multi-hop topologies, in which a donor node – the only node with a direct connection to the 5G Core (5GC) – provides backhaul connectivity to IAB nodes. These nodes can, in turn, act as parent nodes for other IAB nodes or directly serve UEs. Relying on a disaggregated RAN architecture, each IAB node comprises a MT, used to connect upstream to the donor or parent node over the backhaul link, and a Distributed Unit (DU), responsible for providing access

to UEs or downstream child nodes. The Central Unit (CU) is located at the donor node.

Despite its conceptual advantages, IAB faces significant implementation complexity and limited flexibility, which have hindered its large-scale adoption, particularly in highly dynamic scenarios such as vehicular networks. Specifically, mobility procedures are rigid and verbose, additional layers are introduced in the 5G protocol stack, and backhaul handovers, although supported by the standard, remain extremely complex to realize in practice [5].

To address some of the challenges of IAB, 3GPP introduced Mobile Base Station Relay (MBSR) [6], an evolution of IAB designed to support more flexible mobility by adding a dedicated mobile CU to assist IAB nodes when changing their donor. However, MBSR still relies on centralized, full-network control, with resource management tightly coupled to that of the donor, as in conventional IAB architectures. As a result, system complexity remains high, and scalability issues become increasingly pronounced as the number of backhaul hops grows.

In addition to architectural limitations, practical IAB implementations remain scarce. Although several analytical and simulation-based studies have investigated different aspects of IAB [7], [8], experimental frameworks are very limited [9], [10]. Moreover, to the best of our knowledge, IAB nodes are currently available only in the form of experimental or pre-commercial products. The combined architectural complexity and lack of real-world validation appear to be the main obstacle to widespread IAB market deployment.

To overcome these limitations, 3GPP introduced WAB in Release 19. In 2025, WAB was standardized as a topological enhancement for 5G-Advanced (5G-A) [11]. In parallel, Mobile Wireless Access Backhaul (MWAB) was standardized as an architectural enhancement targeting Vehicle-Mounted Relays (VMRs) [12]. Although defined by different Working Groups (WGs), the two technologies share the same architectural foundation, which is described in the next section.

Despite its strong potential, the existing literature on WAB remains limited. Current works primarily discuss WAB as a conceptual enabler for NTN integration in 5G and 5G-Advanced networks [13], [14], without providing physical implementations or experimental validation. To the best of our knowledge, this work presents the first practical multi-band WAB testbed, together with its experimental validation in vehicular and O2I scenarios.

## III. WIRELESS ACCESS BACKHAUL

This section presents the WAB architecture and its fundamental procedures, followed by an overview of representative application scenarios that highlight its applicability to highly dynamic mobile environments.

### A. Architecture

The WAB architecture comprises two communication systems: one for radio access and one for wireless backhaul. These systems can operate in either in-band or out-of-band

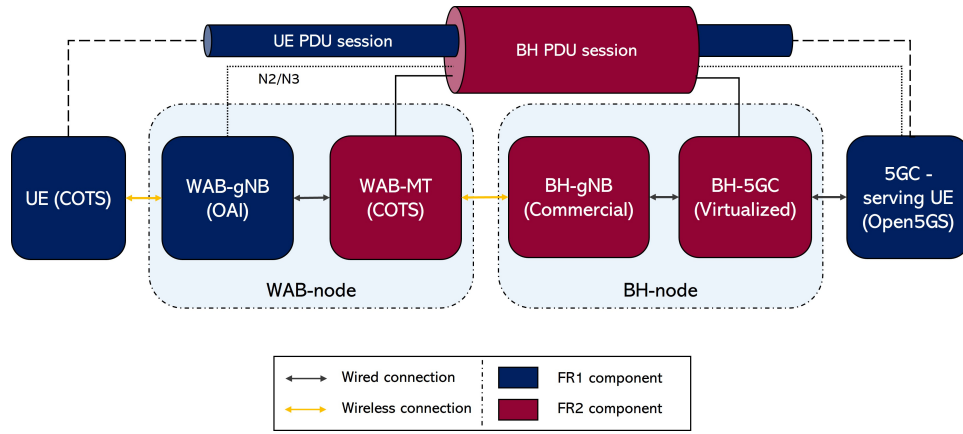


Fig. 1: WAB’s fundamental architecture, including the corresponding elements in the testbed.

configurations, with the objective of providing end-to-end connectivity through wireless backhaul. A schematic representation of the basic architecture is shown in Fig. 1.

One of the core elements of the WAB architecture is the WAB Node, which consists of a WAB-gNB and a WAB Mobile Termination (WAB-MT). The WAB-gNB is a standard-compliant 5G BS that provides radio access to UEs, while the WAB-MT supports a subset of UE functionalities and establishes a wireless connection with the BH-gNB. This connection is used by the WAB-gNB as a backhaul link toward the Core Network (CN), referred to as 5GC-Serving-UE.

Each WAB Node is associated with a donor node, referred to as the BH node, which includes the BH-gNB and a BH-5GC. In the basic configuration, the BH-gNB is also a 5G standard-compliant BS, that provides connectivity to the WAB-MT through conventional radio access procedures and resources. The BH-gNB is locally connected to the BH-5GC, whose N6 interface links to the 5GC-Serving-UE. Alternatively, the backhaul segment can be implemented using a non-3GPP link or network.

In all cases, end UEs remain fully agnostic to the underlying backhaul mechanisms, maintaining full service transparency. This property represents one of the key flexibility features of WAB, enabling the extension of 5G coverage through heterogeneous and non-3GPP infrastructures.

The WAB architecture enables end-to-end connectivity for the end UE by tunneling the N2 and N3 interfaces – linking the WAB-gNB to the 5GC-Serving-UE – over Backhaul (BH) Packet Data Unit (PDU) sessions established between the WAB-MT and the BH-5GC. In the control plane, the wireless backhaul is provided through a BH PDU session that carries the N2 interface between the WAB-gNB and the Access and Mobility Management Function (AMF) of the 5GC-Serving-UE. Similarly, in the user plane, traffic is conveyed over a separate BH PDU session supporting the N3 interface between the WAB-gNB and the User Plane Function (UPF) of the 5GC-Serving-UE.

The backhaul (red in Fig. 1) and access (blue in Fig. 1) segments operate as two logically independent networks. The backhaul network provides backhaul connectivity to the WAB-

MT, while the access network serves the end UE. The backhaul network can be implemented over either a Terrestrial Network (TN) or a NTN; in both cases, 5G access services remain transparent to end UEs, regardless of the underlying backhaul technology.

### B. Basic Procedures

The WAB-node attachment, also referred to as WAB-node integration, begins with the setup of the WAB-MT, which connects to the BH-gNB as a standard UE using conventional 5G access procedures. Once authorized by the BH-5GC, the WAB-MT establishes one or more BH PDU sessions with the UPF of the BH-5GC. Multiple BH PDU sessions can be created to transport different logical interfaces or to enable differentiated traffic handling based on Quality of Service (QoS) requirements. These sessions form the foundation for carrying traffic from the WAB-gNB and its connected UEs.

Following the WAB-MT setup, the WAB-gNB is initialized and registers with the 5GC-Serving-UE, thereby enabling the establishment of PDU sessions for connected UEs. Specifically, each UE PDU session is supported by a Data Radio Bearer (DRB) between the UE and the WAB-gNB, and by a conventional N3 GPRS Tunneling Protocol (GTP) tunnel between the WAB-gNB and the 5GC-Serving-UE. The N3 tunnel is encapsulated within the BH PDU session tunnels established during the WAB-node integration phase.

Through the Xn interface, the WAB-gNB can establish connections with neighboring gNBs. These connections are tunneled through the backhaul network and may terminate either at the BH-gNB serving the WAB-MT or at other gNBs connected to the 5GC-Serving-UE.

As the WAB node moves, the WAB-MT follows legacy UE mobility procedures. This behavior represents one of the key mobility features of WAB, enabling seamless handovers within the backhaul network. Moreover, the WAB-MT can request the establishment or modification of BH PDU sessions based on the traffic requirements of the WAB-gNB as it moves across the network. To prevent multi-hop across mobile WAB nodes, a WAB-MT is not allowed to hand over to a target WAB-gNB. As a result, star-like, single-hop logical topologies

are formed, interconnecting mobile WAB nodes with the donor node. However, this single-hop logical constraint does not restrict the backhaul network itself, which may employ arbitrary underlying technologies or topologies to support the user- and control-plane tunneling required by mobile WAB nodes.

Free mobility and seamless backhaul handovers are the two key features that distinguish the WAB architecture from similar solutions, such as NR femtocells, which are primarily designed to provide NR access in residential or enterprise environments. An important research direction for WAB adoption in mobile and vehicular scenarios is the design of efficient interference management and coordination techniques, as mobile WAB nodes may generate interference when operating within static infrastructures due to imperfect synchronization.

### C. Mobility Applications

Thanks to seamless mobility support and its multi-technology backhaul design, WAB enables highly dynamic urban applications. A WAB node can carry a local 5G access *bubble*, allowing nearby users and vehicles to connect as the node moves through the environment. This capability can be leveraged to provide 5G connectivity on trains or other long-distance transportation systems, where coverage is often intermittent. By deploying a WAB node on board, only the WAB-MT performs handovers when the train moves, while a large number of UEs remain attached to the same serving gNB. This significantly reduces the signaling overhead and core network load, while improving service quality and continuity, even across tunnels or national borders [15].

Similarly, WAB systems can support temporary or emergency deployments, such as disaster recovery scenarios or large-scale public events (e.g., earthquakes, floods, or mobile crowds and city-wide sport events). In these cases, mobile WAB nodes, potentially obtaining backhaul connectivity via NTN, can rapidly extend coverage in areas where traditional terrestrial infrastructures are unavailable or highly congested.

## IV. WAB EXPERIMENTAL FRAMEWORK

The realized testbed aligns with the fundamental architecture of WAB segments and the corresponding components are displayed in Fig. 1 (in brackets). The experimental setup implements a multi-band WAB configuration, where the access segment – connecting UE and WAB-gNB – operates at FR1, while the backhaul segment – connecting WAB-MT and BH-gNB – works at FR2.

A detailed description of the testbed components is provided below, highlighting how they implement a 3GPP-compliant, fully functional WAB system using open-source software and commercial hardware, ensuring compatibility with COTS UEs. The assembly required no hardware modifications beyond standard 5G components. This simplicity is key to achieve rapid and cost-effective deployment, thereby facilitating the widespread adoption of WAB technology.

TABLE I: Operational parameters of BH FR2 components.

Parameter	Value
<b>AAU coordinates (lat, lon, h)</b>	45.478671, 9.232550, 22 m
<b>AAU azimuth, down tilt</b>	135°, 2°
<b>Center frequency</b>	27.2 GHz
<b>Channel bandwidth</b>	200 MHz
<b>Subcarrier spacing</b>	120 kHz
<b>Frame structure</b>	TDD 4:1
<b>Maximum QAM order (D/U)</b>	256/64
<b>AAU TX power</b>	37.5 dBm
<b>AAU gain</b>	32.5 dBm
<b>AAU EIRP</b>	70 dBm
<b>AAU MIMO</b>	8T-8R
<b>CPE gain</b>	20 dBi
<b>CPE EIRP</b>	40 dBm
<b>CPE MIMO</b>	2T-2R

### A. FR2 components

The FR2 segment components are part of the High-Frequency Campus Lab (HFCL) [16], an open and standard-compliant FR2 5G network deployed at Politecnico di Milano. Specifically, the WAB-MT is implemented using a COTS Customer Premises Equipment (CPE). The BH-gNB's Active Antenna Unit (AAU) is installed at a height of 22 m on a building rooftop and is interfaced via a 25 Gbps eCPRI fiber fronthaul to a Base Band Unit (BBU). The BBU is connected to a virtualized commercial 5GC (BH-5GC) through a 10 Gbps backhaul link.

The segment operates at a center frequency of 27.2 GHz, with a channel bandwidth of 200 MHz and a subcarrier spacing of 120 kHz. The frame structure follows a Time Division Duplexing (TDD) 4:1 configuration. The AAU provides an Effective Isotropic Radiated Power (EIRP) of 70 dBm with an 8T8R Multiple Input, Multiple Output (MIMO) configuration, while the CPE operates with an EIRP of 40 dBm and a 2T2R MIMO configuration.

Further details on the FR2 segment are listed in Table I. The FR2 network is used exclusively for research purposes and was entirely dedicated to the testbed, without any additional traffic.

### B. FR1 components

The UE used in the testbed is a COTS 5G smartphone operating in FR1. The WAB-gNB is implemented using an OpenAirInterface (OAI) gNB, deployed on a laptop equipped with an Ettus Universal Software Radio Peripheral (USRP) B210 SDR. OAI is an open-source platform that enables the deployment of a 5G RAN on general-purpose hardware, which can be connected to SDRs to provide wireless access to commercial UEs [17].

The FR1 gNB operates with 40 MHz bandwidth and a subcarrier spacing of 30 kHz in a SISO configuration. The maximum transmission power is 20 dBm, and the TDD configuration follows a 4:1 downlink-to-uplink split. The WAB-gNB laptop is connected to the WAB-MT via an Ethernet link. Finally, the 5GC-Serving-UE consists of an Open5GS Core instance installed on a general-purpose server connected to the BH-5GC. Open5GS is an open-source implementation of the 5GC, composed of virtualized Network Functions.

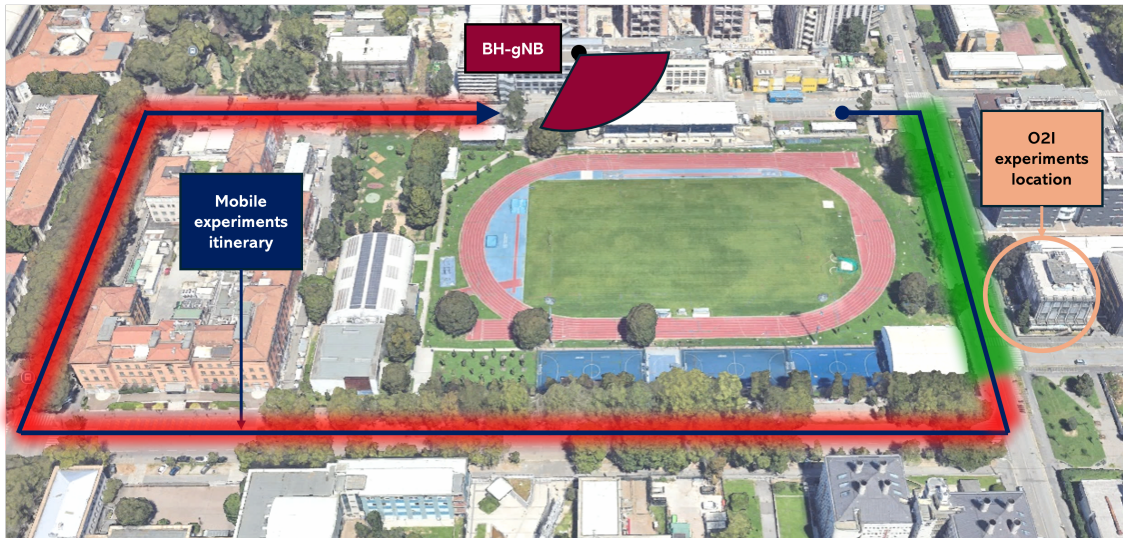


Fig. 2: Aerial view of the urban neighborhood covered by the FR2 BS together with experiment locations. Mobile experiment trajectory shows NLoS and Line of Sight (LoS) regions highlighted, respectively, in red and green.

### C. Connectivity

Once all components were assembled into the final WAB testbed, connectivity was established as follows. Since the 5GC-Serving-UE could not be directly reached by the WAB-gNB due to the CPE Network Address Translation (NAT) mechanism, a Wireguard tunnel was deployed to transport the N2 and N3 interfaces between the 5GC-serving-UE and the WAB-gNB. Wireguard tunnels are open-source Virtual Private Networks (VPNs) that utilize state-of-the-art cryptographic protocols, offering a secure and low-overhead solution. This configuration reflects real-world deployments, where the N2 and N3 interfaces are typically protected from direct exposure to external networks. Some adjustments to the tunnel configuration were required to optimize performance. In particular, the Maximum Transmission Unit (MTU) size was reduced from 1420 bytes to 1384 bytes, as suggested in [18].

In summary, the proposed setup employs three levels of encapsulation to ensure proper end-to-end connectivity: the BH PDU tunnel encapsulates the VPN tunnel transporting the N2 and N3 interfaces, which in turn carries the PDU sessions of the end UEs.

## V. VALIDATION AND RESULTS

Dense urban environments pose significant challenges to high-frequency signals in the FR2 band, where buildings and other obstacles cause severe penetration and propagation losses. Multi-band WAB technology mitigates these effects by jointly exploiting FR2 and FR1 links to extend coverage and improve reliability. In particular, an FR1 hop can overcome blockages that would otherwise disrupt FR2-only connectivity. Moreover, while all UEs support FR1 operation, only a limited subset can directly access FR2 RANs. A mobile WAB system enables transported and nearby FR1 UEs to benefit from the high capacity provided by FR2 backhaul connectivity.

To validate the effectiveness of WAB under these conditions, we conducted an extensive experimental campaign focused

on the operation of a mobile WAB node in a dense urban environment. A fully mobile WAB node was assembled and used to perform measurements while moving through the urban area, within the service region of a single FR2 sector providing backhaul connectivity. In addition, we carried out O2I experiments to complement the mobility evaluation and assess system performance under static yet propagation-challenging conditions.

Figure 2 shows an aerial view of the urban neighborhood where the tests were performed, indicating the placement and orientation of the BH-gNB. In both scenarios, the BH-5GC and 5GC-Serving-UE were located inside the building hosting the BH-gNB, while the WAB node and end UE were moved around the area. The CPE (WAB-MT) was powered by a power bank and connected to a laptop running probe software to collect FR2 link measurements, and via Ethernet to the general-purpose machine running the OAI gNB for FR1 log acquisition through OAI logging functions. A Secure Shell (SSH) tunnel between this machine and the 5GC-Serving-UE server enabled remote execution of *iperf3* commands on both the server and the UE. Speed tests were conducted using Transmission Control Protocol (TCP) connections to evaluate end-to-end throughput.

### A. Mobile experiments

In this scenario, the WAB node was installed on a vehicle, as shown in Figure 3. The WAB-gNB and UE were placed inside the cabin, while the WAB-MT (FR2 CPE) was mounted on the vehicle rooftop. The vehicle moved at up to 30 km/h. Given the high directivity of the CPE antenna array and possible signal losses or reflections from the vehicle body, the WAB-MT was mounted at the rear, with its antenna array oriented perpendicular to the ground. This setup ensured optimal reception when traveling south in the LoS area. A GPS device tracked the route and georeferenced the measurements. The chosen itinerary looped around an outdoor sports center



Fig. 3: Mobile WAB node.

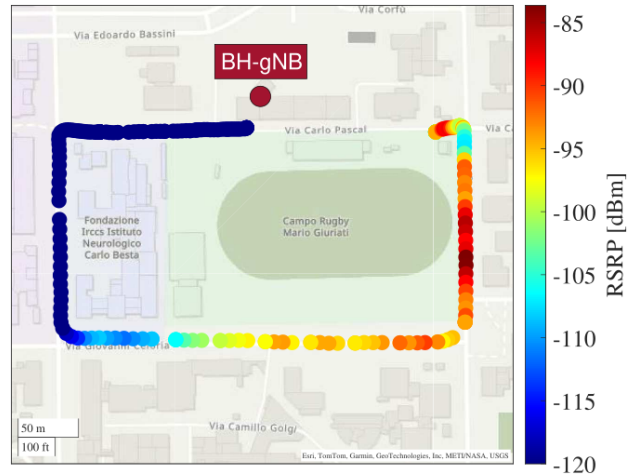
and included segments with trees and buildings causing partial signal obstruction. End-to-end throughput measurements were performed in both Downlink (DL) and Uplink (UL) directions.

We first present the DL results. The data show that the end-to-end throughput (i.e., UE throughput) strongly correlates with the FR2 backhaul link quality. As illustrated in Figure 4, the FR2 backhaul Reference Signal Received Power (RSRP) peaks at  $-83$  dBm in the LoS zone, where the WAB-MT has direct visibility of the BH-gNB. In this region (until 14:45:40, as shown in Figure 5a), the end-to-end throughput reaches approximately 50 Mbps. As the vehicle moves into the NLoS area, performance gradually degrades: throughput begins to decline when a single building obstructs the signal and eventually drops to zero in deep NLoS. This throughput degradation occurs faster than the corresponding decrease in FR2 backhaul RSRP.

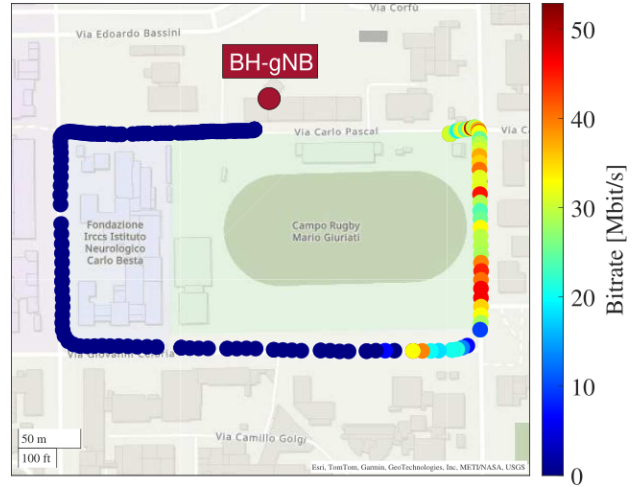
This discrepancy is clarified in Figure 5b: as the end-to-end throughput decreases, the FR2 backhaul link exhibits an increasing Block Error Rate (BLER), explaining the abrupt drop in performance. The figure also reports the serving beams for both Synchronization Signal Block (SSB) and Channel State Information - Reference Signal (CSI-RS). Under LoS conditions, the wider SSB beams remain stable, whereas in NLoS regions, beam switching begins. In contrast, the narrower and more channel-sensitive CSI-RS beams continuously adjust to maintain link quality. Beam switching, however, shows no observable impact on end-to-end throughput.

During the tests, the FR1 access link operated entirely inside the vehicle, where external factors had minimal influence. The Modulation and Coding Scheme (MCS) remained stable around 27 for most of the experiment. In contrast, the FR2 segment faced more challenging conditions, with average MCS values around 20, reflecting the effects of mobility, obstructions, and environmental dynamics on the backhaul link.

UL measurements exhibited a trend similar to the DL results. End-to-end throughput peaked in the LoS region, matching the maximum FR2 backhaul RSRP values, and dropped rapidly as the vehicle entered NLoS. On average, the UL throughput stabilized around 1 Mbps. The notable imbalance between end-to-end DL and UL throughput pri-



(a) DL FR2 RSRP map

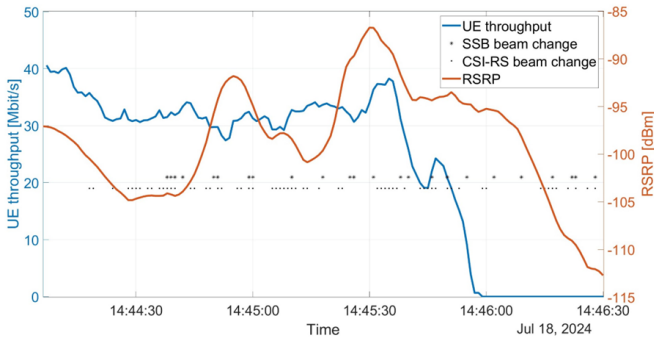


(b) DL end-to-end throughput map

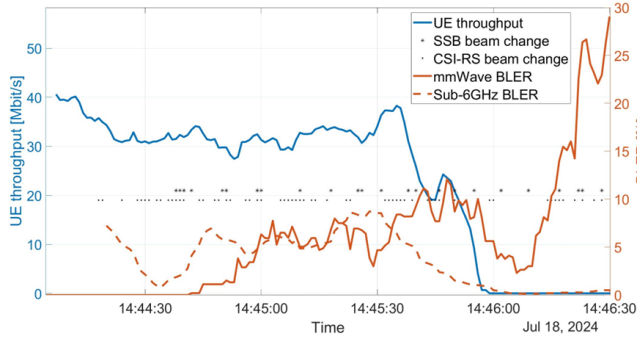
Fig. 4: Mobile WAB measurements of FR2 RSRP and end-to-end throughput.

marily arises from the configuration of the mmWave backhaul segment. This setup is unfavorable for the UL direction: the 4:1 TDD frame prioritizes DL traffic, the CPE transmits at lower power than the AAU, and the maximum supported Quadrature Amplitude Modulation (QAM) order is higher in DL. Additional imbalance stems from the FR1 access segment, whose TDD scheme mirrors that of the FR2 link.

The results from the vehicular experiments demonstrate that reliable FR2 coverage through the WAB architecture can be achieved in LoS scenarios as well as in NLoS conditions where shadowing is not excessively severe. Moreover, the proposed architecture enables widely available COTS FR1 smartphones to access an FR2 RAN without requiring dedicated or costly FR2 radio modules. Due to the limited coverage of the available FR2 network, the testbed could not rely on multiple BH nodes; consequently, an experimental evaluation of backhaul handovers was left outside the scope of this study. Future work will focus on experimentally assessing backhaul handover performance under mobility.



(a) End-to-end throughput, FR2 RSRP and beam changes in mobile WAB experiments.



(b) End-to-end throughput, FR2 and FR1 BLER and beam changes in mobile WAB experiments.

Fig. 5: Mobile WAB experiment results plotted in time.

### B. O2I experiments

In this scenario, the WAB node was placed inside a building with direct visibility of the BH-gNB. End-to-end throughput measurements were conducted at five indoor positions, as shown in Fig. 6. Position 1 corresponds to a LoS condition with the BH-gNB, with only a glass facade attenuating the signal. Positions 2 and 4 are located deeper inside the building but remain subject to glass attenuation only. Positions 3 and 5, situated behind interior walls, experience additional attenuation of the incoming signal.

We first conducted FR2-only speed tests by moving the CPE through each of the five positions to assess the performance of the backhaul link. Subsequently, we assembled the WAB node and placed it at Position 1 to ensure the best possible signal conditions. We then conducted speed tests by moving the final UE, connected to the WAB node via the FR1 link, through each of the five positions. Tests were performed in both the UL and DL directions.

Similarly to the mobile experiments, the directivity of the WAB-MT must be considered. During the FR2 measurements, both with and without the WAB node, the CPE was oriented in the optimal direction, as recommended in [16], to ensure maximum throughput even under NLoS conditions. This reflects the reasonable assumption that any deployed antenna array would be installed with optimal alignment.

To enable a fair comparison between the 200 MHz FR2 CPE-only scenario and the 40 MHz FR1 WAB-gNB config-

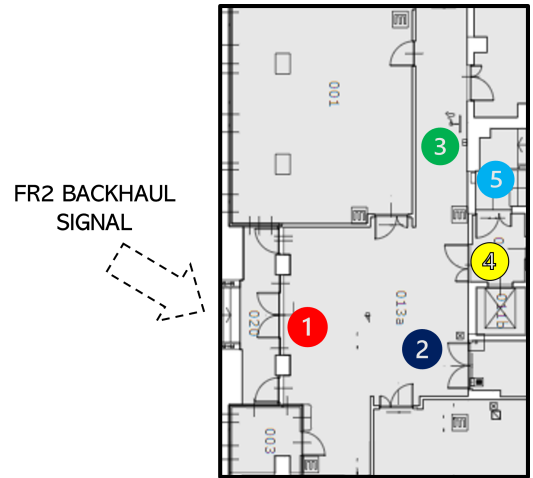
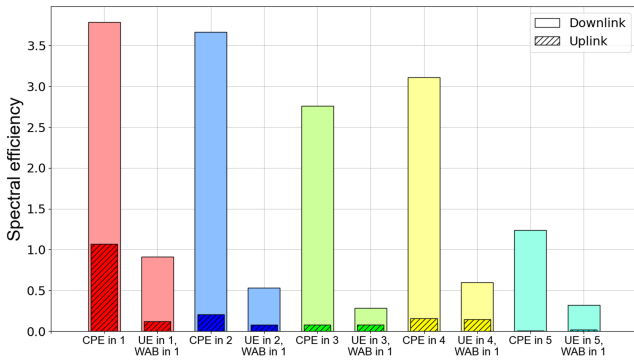


Fig. 6: O2I experiment positions.

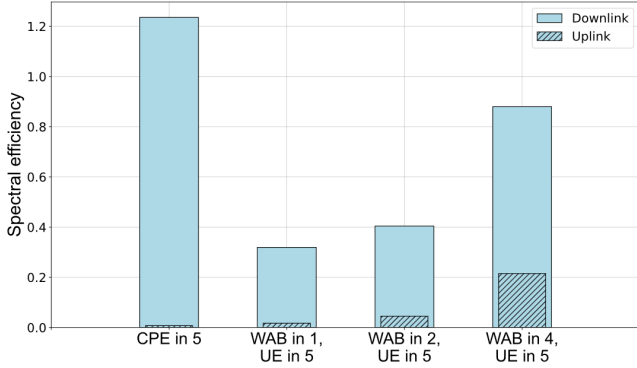
uration, we computed the corresponding spectral efficiency results. However, it is important to note the substantial differences between the two implementations. The FR2 RAN is a commercial, optimized system running on dedicated hardware, operating over a 200 MHz bandwidth with a  $2 \times 2$  MIMO configuration (limited by the CPE), a maximum transmit power of 37.5 dBm, and an antenna gain of 32.5 dBi. In contrast, the FR1 link is a prototype implementation based on virtualized functions running on a general-purpose machine with SDRs, operating in SISO mode with a transmit power of only 20 dBm and a basic dipole antenna. Consequently, a significantly higher spectral efficiency is expected from the FR2 link compared to the FR1 one.

The obtained results are shown in Fig. 7a. In the DL case, as expected, the FR2-only CPE achieves significantly higher spectral efficiency than the WAB system, particularly at Positions 1 and 2, where the signal is attenuated only by glass. In the UL case, FR2 performance degrades sharply when transitioning from LoS to NLoS conditions. The WAB system also exhibits a performance drop between Position 1 and Positions 2 and 4, but the reduction is less pronounced. Notably, at Positions 3 and 5, where additional wall attenuation is present, the WAB system achieves comparable or even higher UL spectral efficiency than the FR2-only CPE. These results highlight the potential of the WAB architecture to mitigate FR2 limitations in challenging indoor NLoS environments, particularly in the uplink. Therefore, we further investigated Position 5, where the WAB system outperformed the FR2 CPE in terms of UL spectral efficiency.

In this additional campaign, the UE was fixed at Position 5, while the WAB node was moved to Positions 2 and 4. This configuration maintained a stable backhaul link while reducing the distance between the WAB node and the UE. This adjustment had a significant impact on the FR1 access link quality, given the limitations of our testbed due to the use of prototype SDRs, the WAB-gNB operating with a low maximum transmit power, and its signal attenuating noticeably with increasing distance.



(a) DL and UL SEs for each measurements positions of O2I experiments. Bar colors correspond to positions colors used in Fig. 6.



(b) DL and UL SEs of the additional indoor campaign.

Fig. 7: O2I experiments spectral efficiencies.

The results, reported in Fig. 7b, show a clear improvement in both DL and UL spectral efficiency as the WAB node is moved closer to the UE, highlighting the influence of access link quality. Despite the limited transmit power of the WAB-gNB, the end-to-end UL spectral efficiency of the WAB system surpasses that achieved by the FR2-only CPE. These findings confirm that the WAB architecture can effectively mitigate the typical limitations affecting FR2 UL transmissions [16], delivering enhanced performance even in challenging NLoS indoor scenarios.

In the DL direction, the end-to-end spectral efficiency of the WAB setup remains lower than that of the FR2-only CPE. This limitation is primarily due to the prototype nature of the WAB-gNB used in our testbed. However, we expect that replacing the current FR1 configuration with a more powerful, commercial-grade FR1 system would significantly enhance downlink performance, potentially allowing the WAB architecture to outperform the FR2-only configuration even in the DL direction.

## VI. CONCLUSIONS & FUTURE WORK

This paper introduced WAB as a promising enabler for mobile base stations and flexible wireless backhaul, as well as an effective approach for exploiting FR2 communications. We presented a WAB testbed that addresses the current lack of experimental validation in the literature and provides a practical foundation for further research.

Through an extensive experimental campaign conducted in both mobile and O2I scenarios, the proposed framework, based on commercial hardware and open-source software, demonstrated the feasibility and benefits of multi-band WAB operation. In particular, the combination of FR1 access and FR2 backhaul proved effective in extending coverage and improving reliability under mobility and challenging propagation conditions. The use of standard 5G interfaces, together with the flexibility and multi-technology backhaul support of the WAB architecture, makes it a compelling solution for vehicular and next-generation wireless networks.

We are currently working on extending the proposed testbed to better assess backhaul handover, improve interference and resource management strategies, and integrate additional backhaul technologies to further enhance scalability and performance.

## REFERENCES

- [1] S. Rangan *et al.*, "Millimeter-Wave Cellular Wireless Networks: Potentials and Challenges," *Proceedings of the IEEE*, vol. 102, no. 3, pp. 366–385, 2014.
- [2] L. Finarelli, F. Dressler, M. A. Marsan, and G. Rizzo, "Mobile Networks on the Move: Optimizing Moving Base Stations Dynamics in Urban Scenarios," in *2024 IEEE Vehicular Networking Conference (VNC)*, 2024, pp. 101–104.
- [3] X. Lin, "The Bridge Toward 6G: 5G-Advanced Evolution in 3GPP Release 19," *IEEE Communications Standards Magazine*, vol. 9, no. 1, pp. 28–35, 2025.
- [4] M. Polese *et al.*, "Integrated Access and Backhaul in 5G mmWave Networks: Potential and Challenges," *IEEE Communications Magazine*, vol. 58, no. 3, pp. 62–68, 2020.
- [5] V. F. Monteiro *et al.*, "Paving the Way Toward Mobile IAB: Problems, Solutions and Challenges," *IEEE Open Journal of the Communications Society*, vol. 3, pp. 2347–2379, 2022.
- [6] C.-K. Wen *et al.*, "Shaping a Smarter Electromagnetic Landscape: IAB, NCR, and RIS in 5G Standard and Future 6G," *IEEE Communications Standards Magazine*, vol. 8, no. 1, pp. 72–78, 2024.
- [7] M. Polese *et al.*, "End-to-End Simulation of Integrated Access and Backhaul at mmWaves," in *2018 IEEE 23rd International Workshop on Computer Aided Modeling and Design of Communication Links and Networks (CAMAD)*, 2018, pp. 1–7.
- [8] E. Moro *et al.*, "Toward Open Integrated Access and Backhaul with O-RAN," in *2023 21st Mediterranean Communication and Computer Networking Conference (MedComNet)*, 2023, pp. 61–69.
- [9] T. Tian *et al.*, "Field Trial on Millimeter Wave Integrated Access and Backhaul," in *2019 IEEE 89th Vehicular Technology Conference (VTC2019-Spring)*, 2019, pp. 1–5.
- [10] R. Mundlamuri *et al.*, "Integrated Access and Backhaul in 5G with Aerial Distributed Unit using OpenAirInterface," 2023. [Online]. Available: <https://arxiv.org/abs/2305.05983>
- [11] 3GPP, "Study on additional topological enhancements for NR," 3GPP, TR 38.799, version 19.0.0, 09 2024.
- [12] 3GPP, "Study on architecture enhancements for vehicle-mounted relays - Phase 2," 3GPP, TR 23.700-06, version 19.0.0, 2024.
- [13] S. Zhang *et al.*, "6G for Connected Sky: Holistic Adaptive Combined Airspace and Non Terrestrial Network Architecture," *IEEE Wireless Communications*, vol. 32, no. 5, pp. 204–211, 2025.
- [14] A. Rago *et al.*, "Innovative Multi-Layer Approaches for 6G Integrated Terrestrial and Non-Terrestrial Networks," *IEEE Communications Standards Magazine*, vol. 9, no. 2, pp. 39–47, 2025.
- [15] S. Jaffry *et al.*, "A comprehensive survey on moving networks," *IEEE Communications Surveys & Tutorials*, vol. 23, no. 1, pp. 110–136, 2021.
- [16] M. Morini *et al.*, "Exploring Upper-6GHz and mmWave in Urban 5G Networks: A Direct on-Field Comparison," *IEEE Transactions on Mobile Computing*, pp. 1–14, 2025.
- [17] F. Kaltenberger *et al.*, "OpenAirInterface: Democratizing Innovation in the 5G Era," *Computer Networks*, vol. 176, p. 107284, 05 2020.
- [18] [Online] Available: <https://gist.github.com/nitred/f16850ca48c48c79bf422e90ee5b9d95>.